

Open heavy-flavour measurements in Pb–Pb collisions with ALICE at the LHC

André Mischke*^{a,b} for the ALICE Collaboration

^a *Institute for Subatomic Physics, Department for Physics and Astronomy and EMMEφ, Faculty of Science, Utrecht University, Princetonplein 1, 3584 CS Utrecht, the Netherlands*

^b *School of Physics and Astronomy, University of Birmingham, Birmingham B15 2TT, UK*

E-mail: andre.mischke@cern.ch

The ALICE experiment has measured charm and beauty production in Pb–Pb collisions at $\sqrt{s_{NN}} = 2.76$ TeV and 5.02 TeV, via the reconstruction of hadronic D-meson decays and semi-leptonic D- and B-meson decays. In this contribution, an overview is given on current open heavy-flavour results from ALICE ranging from the nuclear modification factor to elliptic flow measurements and on the interpretation of the data by comparing with different model calculations of in-medium energy loss.

*55th International Winter Meeting on Nuclear Physics
23-27 January 2017
Bormio, Italy*

*Speaker.

1. Introduction

Strongly interacting matter at extreme conditions (temperatures and/or high densities) can be created and studied under laboratory conditions in collisions of heavy atomic nuclei at high energies. Lattice QCD predicts a phase transition from hadronic matter to a deconfined state, the quark-gluon plasma [1]. Heavy quarks (charm and beauty) provide particular good probes for the study of the quark-gluon plasma state and its evolution since they are predominantly produced in initial hard partonic scattering processes in the early stages of the collision. Thanks to the large mass, the charm and beauty p_T -differential cross sections can be calculated perturbatively in Quantum Chromodynamics. In heavy-ion collisions, the heavy quarks pass through the plasma and interact with it through medium-induced gluon radiation (radiative energy loss) and collisions with the plasma constituents (collisional energy loss). The radiative parton energy loss depends on the medium properties, such as the density, temperature and mean free path, which is usually quantified in the so-called transport coefficient \hat{q} . In addition, it depends on the path length in the medium and the parton properties, such as the colour charge and mass [2]. Theoretical models predict [3, 4] that heavy quarks should experience a smaller energy loss than light quarks while propagating through the plasma due to the suppression of small-angle gluon radiation, the so-called *dead-cone effect*. Thus, the measurement of open heavy-flavour production in heavy-ion collisions allows one to study the dynamical properties of the plasma phase, such as the drag and diffusion coefficients.

A comprehensive overview of the recent theoretical and experimental results can be found in [5, 6]. In this contribution, recent results are presented on open charm and beauty production measurements in lead-lead collisions from the ALICE experiment. The results in proton-proton and proton-lead collisions are shown in [7]. Open and hidden heavy-flavour results from ALICE were discussed in [8] at this conference.

Nuclear effects are quantified using the nuclear modification factor R_{AA} where the particle yield in nucleus-nucleus collisions is normalised by the yield in pp interactions, scaled by the averaged number of binary collisions. The latter is obtained from Glauber calculations. A R_{AA} equal to unity would indicate that no nuclear effects, neither "cold" (such as Cronin, shadowing or gluon saturation) nor "hot" (parton energy loss) are present and that nucleus-nucleus collisions can be considered as an incoherent superposition of nucleon-nucleon interactions. The comparison of the nuclear modification factor of charged pions ($R_{AA}^{\pi^\pm}$), mostly originating from gluon fragmentation, with that of charm R_{AA}^D and beauty hadrons R_{AA}^B allows the study of the colour charge and mass dependence of the energy loss. Thus, an ordering pattern of $R_{AA}^{\pi^\pm} < R_{AA}^D < R_{AA}^B$ is expected [9].

2. Experimental setup, trigger and data samples

Since 2010, the Large Hadron Collider (LHC) at CERN provides lead-lead collisions at an unprecedented energy of 2.76 TeV and 5.02 TeV per nucleon-nucleon pair. ALICE is the dedicated experiment at the LHC for the measurements of heavy-ion collisions [10]. Its detector allows for measuring charged particles down to very low p_T (> 100 MeV/c) and has excellent particle identification and vertexing capabilities in a high particle multiplicity environment. At mid-rapidity, tracking with up to 159 three-dimensional space-points and particle identification through the measurement of the specific ionisation energy loss (dE/dx) is performed using the large volume

(90 m³) Time Projection Chamber (TPC), located inside a large solenoidal magnet with a field strength of $B = 0.5$ T. The TPC has a pseudo-rapidity coverage of $|\eta| < 0.9$ and 2π in azimuth. The relative dE/dx resolution is 5-6%. The Time Of Flight (ToF) detector has an intrinsic time resolution of 80 ps and provides pion/kaon separation at 3-sigma level up to about $p_T = 2$ GeV/c. The Inner Tracking System consists of six concentric cylindrical layers of silicon detectors and provides excellent reconstruction of displaced vertices with a transverse track impact-parameter resolution better than $70 \mu\text{m}$ for $p_T > 1$ GeV/c [11]. The total material budget for radial tracks in the transverse plane is $\approx 7.7\%$ of the radiation length. Electron identification at $p_T > 0.5$ GeV/c is performed with the TPC, ToF, Electromagnetic Calorimeter (EMCal), and the Transition Radiation Detector (TRD). The EMCal is a Pb-scintillator sampling calorimeter, located at a radial distance of about 4.5 m from the beam line. The full detector covers the pseudorapidity range $-0.7 < \eta < 0.7$ with an azimuthal acceptance of $\Delta\phi = 107^\circ$. The calorimeter is of the "Shashlik" type built from alternating lead and scintillator segments of 1.44 mm and 1.76 mm thickness, respectively, together with longitudinal wavelength-shifting fibres for light collection. The tower size of the EMCal is approximately 0.014×0.014 rad in $\Delta\phi \times \Delta\eta$, and the depth corresponds to $20.1 X_0$. From electron test beam data, the energy resolution of the EMCal was determined to be $1.7 \oplus 11.1/\sqrt{E(\text{GeV})} \oplus 5.1/E(\text{GeV})\%$ [10]. The TRD is segmented in 18 individual super-modules and provides good separation of electrons from pions for momenta above 1 GeV/c. At forward rapidity ($-4 < \eta < -2.5$), muons are identified with the muon spectrometer, which is composed of two absorbers, a dipole magnet with a field integral of 3 Tm, and tracking and trigger chambers. Tracking is performed by means of five tracking chambers with an intrinsic spatial resolution better than $100 \mu\text{m}$.

The Pb–Pb data were collected at a centre-of-mass energy of $\sqrt{s_{\text{NN}}} = 2.76$ and 5 TeV with a minimum-bias trigger, based on the information of the V0 scintillator hodoscopes ($2.8 < \eta < 5.1$ and $-3.7 < \eta < -1.7$). The efficiency for triggering hadronic interactions was 100% for Pb–Pb collisions in the centrality range considered in the analyses. Beam background collisions were removed offline based on the timing information from the VZERO and Zero Degree Calorimeters, which are located near the beam pipe at $z = \pm 114$ m from the interaction point. Only events with a vertex position within 10 cm from the centre of the detector along the beam line were considered for the analyses. The Pb–Pb data are classified based on their centrality defined in terms of percentiles of the hadronic Pb–Pb cross section and determined from the distribution of the summed amplitudes in the VZERO detector. This distribution was fitted using the Glauber model for the geometrical description of the nuclear collision together with a two-component model for particle production [12]. The integrated luminosity for the $\sqrt{s_{\text{NN}}} = 2.76$ TeV data taking was $10 \mu\text{b}^{-1}$ and 0.1nb^{-1} for the year 2010 and 2011, respectively, and $202.3 \mu\text{b}^{-1}$ for the muon triggered events recorded in 2015 at $\sqrt{s_{\text{NN}}} = 5.02$ TeV.

3. Detection of open heavy-flavour signals

In this section, a brief description of the reconstruction technique for D mesons and heavy-flavour decay leptons is given.

3.1 D mesons

D^0 , D^{*+} and D^+ mesons are reconstructed at mid-rapidity ($|y| < 0.5$) through their exclusive hadronic decays into $D^0 \rightarrow K^- \pi^+$ (BR = $(3.88 \pm 0.05)\%$), $D^{*+} \rightarrow D^0 \pi^+$ (BR = $(67.7 \pm 0.5)\%$) and $D^+ \rightarrow K^+ \pi^- \pi^+$ (BR = $(9.13 \pm 0.19)\%$) [13], based on their decay topology and the invariant mass method. The silicon Inner Tracking System provides excellent impact parameter resolution allowing for isolation of decay products of longer living particles. The impact parameter resolution is well described in Monte Carlo simulations [11]. In addition, kaon and pion identification is performed using TPC and TOF to reduce the background at low p_T .

3.2 Heavy-flavour decay leptons

Leptons are studied through their semi-leptonic heavy-flavour decay charm \rightarrow lepton + X (BR = 9.6%) and beauty \rightarrow lepton + X (BR = 10.9%) [13]. Here, heavy-flavour decay electrons are identified at mid-rapidity with the EMCal and TPC+TOF, where the background, mainly from γ conversion electrons in the detector material and π^0 Dalitz decays, is subtracted from the inclusive electron spectrum on a statistical basis using a cocktail of background electrons and the invariant mass method.

Muons at forward rapidities ($-4 < \eta < -2.5$) are studied with the muon spectrometer. The extraction of the heavy-flavour contribution from the inclusive single muon spectra requires the subtraction of three main background sources: a) muons from the decay-in-flight of light hadrons (decay muons); b) muons from the decay of hadrons produced in the interaction with the front absorber (secondary muons); c) punch-through hadrons. The last contribution can be efficiently rejected by requiring the matching of the reconstructed tracks with the tracks in the trigger system. The background muons have a softer p_T distribution than the heavy-flavour muons, and dominate the low- p_T region. Therefore, the analysis is restricted to the p_T range 2–20 GeV/c. Monte Carlo simulations and a cocktail tuned on data have been used to estimate the contribution from secondary muons, which is small (about 3%) in this p_T range, and to subtract the main source of background of decay muons (about 25%).

4. Results on D-meson measurements

Figure 1 shows the p_T dependence of the nuclear modification factor of prompt D mesons at mid-rapidity in Pb–Pb collisions at $\sqrt{s_{NN}} = 2.76$ TeV [14]. The D-meson yield for the most central events is strongly suppressed (by factor of ≈ 5 at around 10 GeV/c). Energy-loss models describe the trend of the observed suppression at high transverse momentum reasonably well. Furthermore, ALICE studied the R_{AA} of D_s^+ mesons [15] in nucleus-nucleus collisions (cf. Fig. 1). The D_s^+ meson is of particular interest since it is a charm-anti-strange quark state. Earlier measurements have shown that strangeness production is enhanced in nucleus-nucleus collisions. So, one would expect that the strange D-meson yield at intermediate transverse momentum should be enhanced if charm hadronises via recombination in the medium. Model calculations show [16] that the difference between the R_{AA} of D and D_s^+ mesons should be about a factor of 2 for $p_T < 5$ GeV/c (cf. Fig. 1). The ALICE data do not give evidence for a difference within the current statistical and systematic uncertainties.

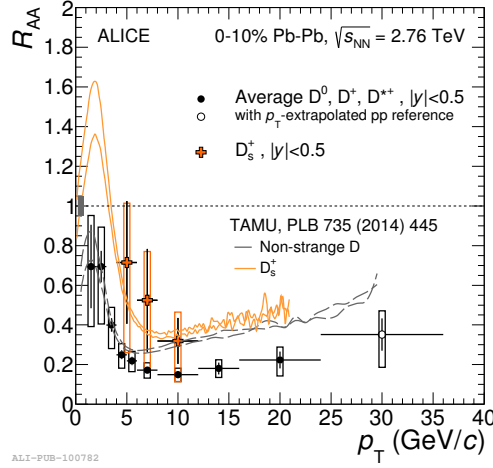


Figure 1: Average of nuclear modification factor R_{AA} of prompt D [14] and D_s^+ mesons [15] at mid-rapidity in the 10% most central Pb–Pb collisions at $\sqrt{s_{NN}} = 2.76$ TeV, compared with the TAMU energy loss model [16].

The prompt D-meson R_{AA} is depicted in Fig. 2 for two different centrality classes together with the charged particles and charged pions R_{AA} . The D-meson yields at $5 < p_T < 10$ GeV/c are suppressed to the same level as observed for light-quark hadrons [15]. The increasing trend of the yield at high transverse momentum can be understood in terms of the hardening of the initial particle spectrum. There is a hint that prompt D mesons are less suppressed than light-quark hadrons at low transverse momentum but the current statistical and systematic uncertainties do not allow for a conclusive interpretation of the data.

The centrality dependence of prompt D-meson R_{AA} [17] is depicted in Fig. 3 together with the R_{AA} of J/ψ from beauty decays measured by CMS (non-prompt J/ψ) [18]. The data indicate that the D-meson R_{AA} is smaller than the J/ψ R_{AA} : this, considering the typical p_T range of B mesons decaying to J/ψ with a p_T in the measured range, can be considered as an indication for a stronger

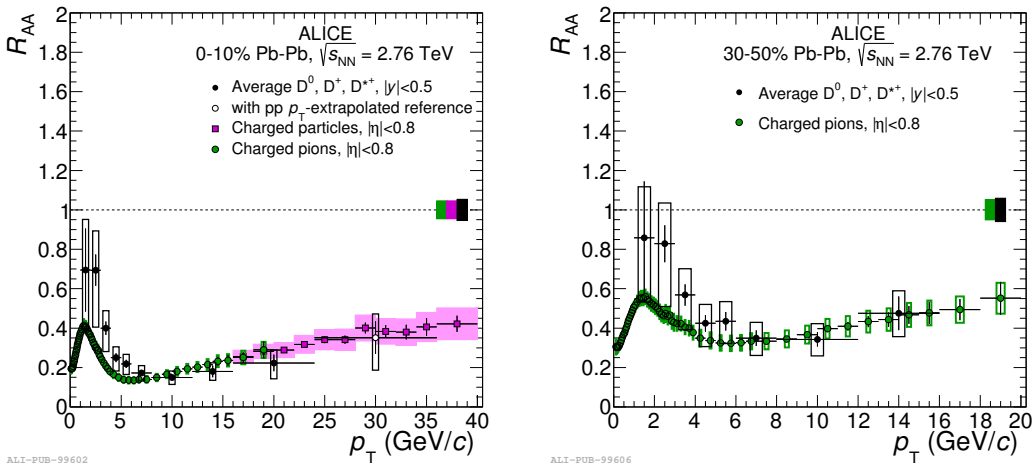


Figure 2: Prompt D-meson and charged pion (charged hadron for $p_T > 20$ GeV/c) R_{AA} at mid-rapidity in the 10% most central Pb–Pb collisions (left panel) and the centrality class 30-50% at $\sqrt{s_{NN}} = 2.76$ TeV [14].

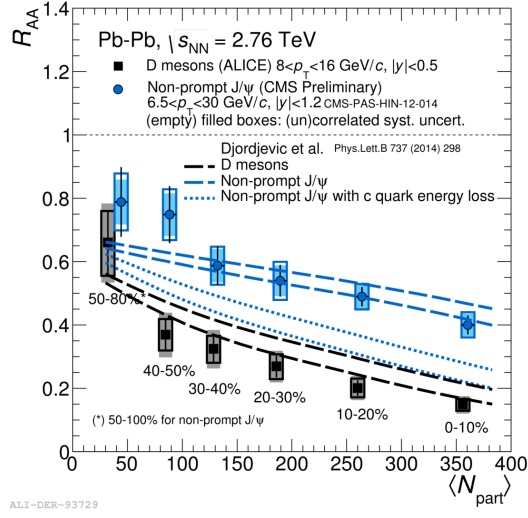


Figure 3: R_{AA} of prompt D mesons [17] and J/ψ from beauty decays [18] versus the number of participating nucleons.

suppression for D mesons than B mesons. This is expected by model calculations including quark-mass dependent energy loss. However, there remains an uncertainty from the comparison in a proper kinematical range. This urges the need for the measurement of fully reconstructed B mesons in heavy-ion collisions over a broad kinematical range at low p_T .

A quantitative understanding of the heavy-ion data in terms of parton energy loss makes it important to disentangle hot nuclear matter from cold nuclear matter effects from the initial state, which arise from the nuclear modification of the parton distribution functions (shadowing),

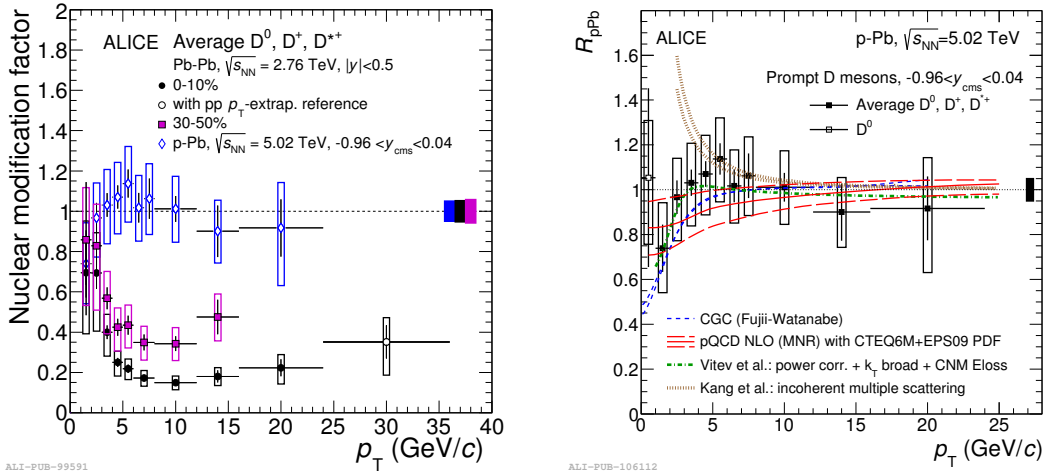


Figure 4: Left panel: R_{pPb} of the average, prompt D meson versus p_T in minimum bias p–Pb collisions at $\sqrt{s_{NN}} = 5.02$ TeV [23] together with the prompt D-meson R_{AA} in Pb–Pb collisions at $\sqrt{s_{NN}} = 2.76$ TeV for two different centrality classes. Right panel: prompt D-meson R_{AA} , compared with models with cold nuclear matter effects only [24, 25]. See text for detailed discussion.

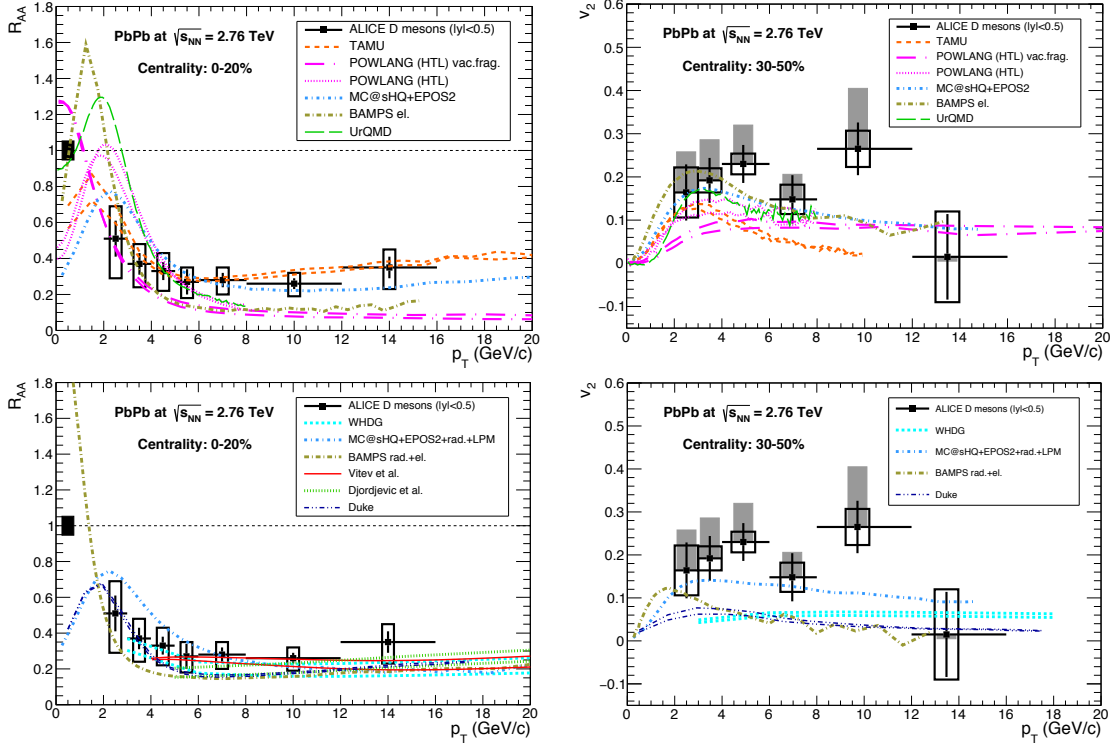


Figure 5: The R_{AA} and elliptic flow parameter v_2 , compared to different energy-loss model calculations, ones with collisional energy loss only (upper panels) and ones with collisional and radiative energy loss (lower panels) [6].

gluon saturation, k_T broadening and Cronin enhancement from multiple parton scatterings, and initial-state energy loss [19, 20, 21, 22]. Initial-state effects can be studied in proton-lead collisions. The nuclear modification factor R_{pPb} of prompt D mesons in p–Pb collisions at $\sqrt{s_{NN}} = 5.02$ TeV [23], shown in Fig. 4, is compatible with unity within systematic uncertainties over the measured p_T range. Thus, the strong suppression of the D-meson yield observed in central Pb–Pb collisions, shown on the left hand panel, is a final-state effect arising from the energy loss of the charm quarks in the plasma. The data are consistent with predictions from models considering cold nuclear matter (CNM) effects only, specifically shadowing [24] and colour-glass condensate models [25] (c.f. Fig. 4, right panel).

Measurements of the particles’ azimuthal momentum distribution and comparison with hydrodynamic model calculations have shown that the outward steaming particles move collectively, with the patterns arising from variations of pressure gradients early after the collision. This parameter characterising this anisotropy is the coefficient of the second-order harmonic of the Fourier decomposition of the azimuthal distribution, called elliptic flow. The study of the azimuthal anisotropy of heavy-quark particles is particularly interesting as it provides information on the degree of thermalisation of heavy quarks in the plasma. Measurements of the azimuthal anisotropy of prompt D mesons (cf. Fig. 5, right panels) and muons from heavy-flavour decays (cf. Fig. 8, right panel) in mid-central Pb–Pb collisions suggest a sizeable elliptic flow of heavy quarks in the plasma. The

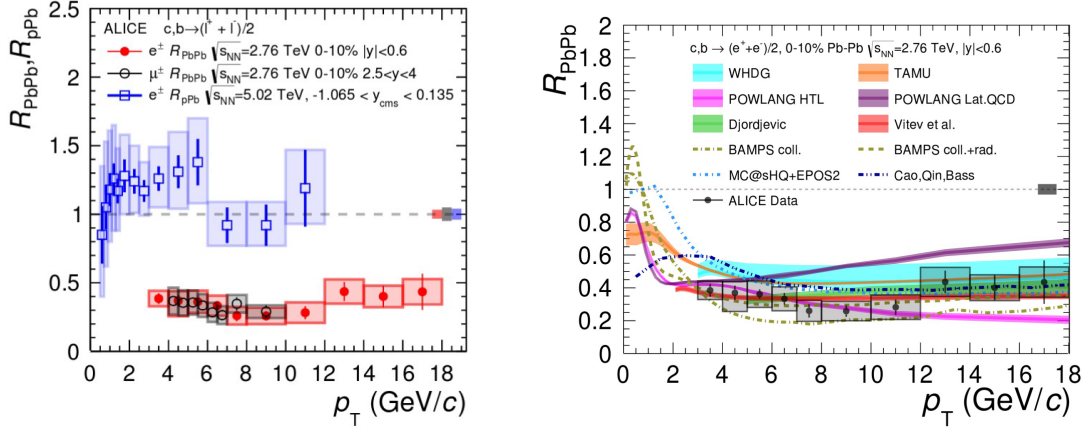


Figure 6: Left panel: R_{AA} of heavy-flavour decay electron and muons in most 10% central Pb–Pb collisions at $\sqrt{s_{NN}} = 2.76$ TeV. The blue symbols illustrate the R_{pPb} for single electrons in minimum bias proton-lead collisions at $\sqrt{s_{NN}} = 5.02$ TeV [28]. Right panel: the single electron R_{AA} is compared with different energy-loss model calculations.

R_{AA} and elliptic flow parameter v_2 are compared simultaneously to different energy-loss model calculations, considering collisional energy loss only (upper panels) or considering collisional and radiative energy loss (lower panels). More precision data are needed to draw strong conclusions. LHC data with different observables will allow to challenge model calculations. Heavy-flavour tagged correlations as well as charm production in jets may add sensitivity to disentangle the different energy loss mechanisms (radiative versus collisional energy loss) and to study how the energy is redistributed within the jet cone and how the energy is dissipated into the plasma [26]. The azimuthal correlations of D mesons and charged particles were measured for the first time with the ALICE detector in pp collisions at $\sqrt{s} = 7$ TeV and p–Pb collisions at $\sqrt{s_{NN}} = 5.02$ TeV [27]. The studies on the production of jets with D mesons are ongoing.

5. Results on single leptons

The nuclear modification factors of single electrons at mid-rapidity in Pb–Pb and p–Pb collisions and single muons at forward rapidity in Pb–Pb collisions are depicted in Fig. 6. Their yields are suppressed to about the same level as observed for prompt D mesons. The R_{pPb} for single electrons in minimum bias proton-lead collisions at $\sqrt{s_{NN}} = 5.02$ TeV [28] however is compatible with unity over the full measured p_T range within systematic uncertainties. The heavy-flavour decay electron results for $|\eta| < 0.6$ in the most 10% central Pb–Pb collisions are compared with different energy-loss model calculations in the right panel of Fig. 6. The agreement is relatively good in the measured p_T range, although POWLANG (Lat. QCD) seems to over-predict the data.

The single muon R_{AA} at forward rapidities in the 10% most central Pb–Pb collisions at $\sqrt{s_{NN}} = 5.02$ TeV as a function of p_T and number of participants is depicted in Fig. 7 [29]. The data agree with previous measurements in the same centrality class and at lower collision energy.

In Fig. 8, the R_{AA} and elliptic flow v_2 parameter of single muons in Pb–Pb collisions at $\sqrt{s_{NN}} = 2.76$ TeV are simultaneously compared to energy-loss model calculations [30], which describe the data reasonably well.

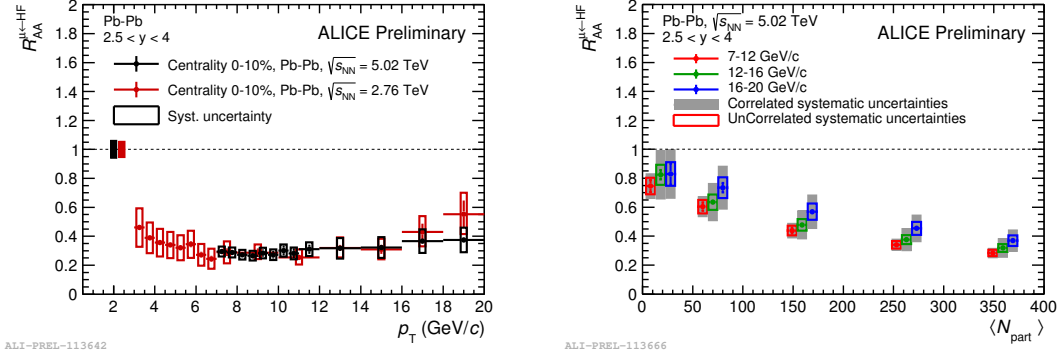


Figure 7: R_{AA} of single muons at forward rapidities in the 10% most central Pb–Pb collisions at $\sqrt{s_{NN}} = 5.02$ TeV as a function of p_T (left panel) and number of participants (right panel) [29].

6. Summary

ALICE has measured prompt D mesons and heavy-flavour electrons and muons in Pb–Pb collisions at $\sqrt{s_{NN}} = 2.76$ and 5.02 TeV at the CERN-LHC. In this contribution, recent results on the nuclear modification factor and the azimuthal anisotropy of open heavy-flavour were presented. It was found that the yields of both D mesons and leptons are strongly suppressed at high p_T (>6 GeV/c) in the 10% most central Pb–Pb collisions. This provides more insight into the energy-loss mechanisms for heavy quarks. Moreover, D mesons exhibit a non-zero elliptic flow, suggesting strong re-interactions of charm quarks within the medium, which was also observed for the J/ψ [31].

The ultimate goal is to constrain the transport properties of the plasma, such as the drag and diffusion coefficient, and the degree of thermalisation of heavy quarks in the plasma. Heavy-flavour correlations measurements might help to disentangle the different energy-loss mechanisms (radiative versus collisional energy loss). Further precision measurements in an extended p_T range, which will be available after the detector upgrades and the expected increase in luminosity in run-3, are needed to further constrain theoretical model calculations. The results from the p–Pb data taking in 2016 at $\sqrt{s_{NN}} = 5.02$ and 8.16 TeV will allow to further understand in detail the cold nuclear matter effects.

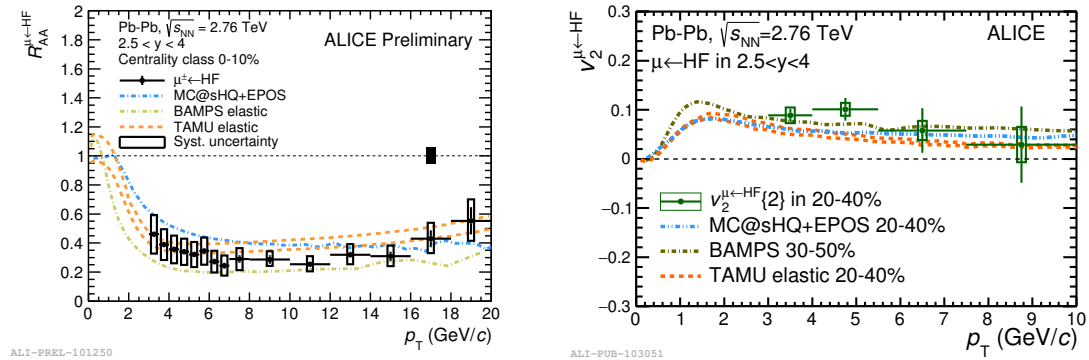


Figure 8: R_{AA} and elliptic flow v_2 parameter of single muons in Pb–Pb collisions at $\sqrt{s_{NN}} = 2.76$ TeV, compared with different energy-loss models [30].

Acknowledgments

I would like to thank the organisers for the invitation and the inspiring atmosphere during the conference. This work was supported by the Netherlands Organisation for Scientific Research (project number: 680-47-232) and the Dutch Foundation for Fundamental Research (project numbers: 12PR3083).

References

- [1] A. Borsanyi et al, Phys. Lett. B 730, 99 (2014).
- [2] R. Baier et al., Nucl. Phys. B 483, 291 (1997).
- [3] Y.L. Dokshitzer and D.E. Kharzeev, Phys. Lett. B 519, 199 (2001).
- [4] M. Djordjevic, M. Gyulassy and S. Wicks, Phys. Rev. Lett. 94, 112301 (2005).
- [5] G. Aarts *et al.*, Eur. Phys. J. A 53, 93 (2017).
- [6] A. Andronic *et al.*, Eur. Phys. J. C 76, 107 (2016).
- [7] J. Norman (for the ALICE Collaboration), these proceedings.
- [8] J. Stachel, these proceedings.
- [9] S. Wicks, W. Horowitz, M. Djordjevic, M. Gyulassy, Nucl. Phys. A784, 426 (2007).
- [10] ALICE Collaboration, J. Instrum. **3**, S08002 (2008).
- [11] ALICE Collaboration, J. Instrum. **5**, P03003 (2010).
- [12] ALICE Collaboration, Phys. Rev. Lett. **105**, 252301 (2010).
- [13] C. Patrignani *et al.* (Particle Data Group), Chin. Phys. C, 40, 100001 (2016) and 2017 update.
- [14] ALICE Collaboration, JHEP 1603, 081 (2016) and JHEP 09, 112 (2012).
- [15] ALICE Collaboration, JHEP 1603, 082 (2016).
- [16] M. He, R.J. Fries and R. Rapp, Phys. Lett. B 735, 445 (2014).
- [17] ALICE Collaboration, JHEP 11, 205 (2015).
- [18] CMS Collaboration, CMS-PAS-HIN-12-014 and CMS-PAS-HIN-15-005.
- [19] C.A. Salgado et al., J. Phys. G 39, 015010 (2012).
- [20] J.W. Cronin et al., Phys. Rev. D 11, 3105 (1975).
- [21] A. Accardi, hep-ph/0212148.
- [22] R.C. Hwa and C. Yang, Phys. Rev. Lett. 93, 082302 (2004).
- [23] ALICE Collaboration, Phys. Rev. C 94, 054908 (2016) and Phys. Rev. Lett. 113, 232301 (2014).
- [24] K.J. Eskola, H. Paukkunen, C.A. Salgado, JHEP 0904, 65 (2009).
- [25] H. Fujii and K. Watanabe, Nucl Phys. A 920, 78 (2013).
- [26] M. Nahrgang, J. Aichelin, P. B. Gossiaux, and K. Werner, Phys. Rev. C 90, 024907 (2014).
- [27] ALICE Collaboration, Eur. Phys. J. C 77, 245 (2017).
- [28] ALICE Collaboration, Phys. Lett. B 771, 467 (2017).
- [29] ALICE Collaboration, Phys. Rev. Lett. 109, 112301 (2012).
- [30] ALICE Collaboration, Phys. Lett. B753, 41 (2016).
- [31] Mohamad Tarhini (for the ALICE Collaboration), Quark Matter 2017, proceeding in preparation.